Published in final edited form as:
Nanomedicine (Lond). 2013 October ; 8(10): 1601–1609. doi:10.2217/nnm.12.165.

Gold nanoparticle imaging and radiotherapy of brain tumors in mice

James F Hainfeld[*,‡,1], **Henry M Smilowitz**[‡,2], **Michael J O'Connor**[1], **Farrokh Avraham Dilmanian**[3,4], and **Daniel N Slatkin**[1]

[1]Nanoprobes, Inc., 95 Horseblock Road, Unit 1 Yaphank, NY 11980, USA

[2]Department of Cell Biology, Room L-2018, University of Connecticut Health Center, 263 Farmington Avenue, Farmington, CT 06030, USA

[3]Medical Department Brookhaven National Laboratory, Upton, NY 11973, USA

[4]Departments of Radiation Oncology & Neurology, State University of New York at Stony Brook, Health Sciences Center, Level 2, Stony Brook, NY 11794-7028, USA

Abstract

Aim—To test intravenously injected gold nanoparticles for x-ray imaging and radiotherapy enhancement of large, imminently lethal, intracerebral malignant gliomas.

Materials & methods—Gold nanoparticles approximately 11 nm in size were injected intravenously and brains imaged using microcomputed tomography. A total of 15 h after an intravenous dose of 4 g Au/kg was administered, brains were irradiated with 30 Gy 100 kVp x-rays.

Results—Gold uptake gave a 19:1 tumor-to-normal brain ratio with 1.5% w/w gold in tumor, calculated to increase local radiation dose by approximately 300%. Mice receiving gold and radiation (30 Gy) demonstrated 50% long term (>1 year) tumor-free survival, whereas all mice receiving radiation only died.

Conclusion—Intravenously injected gold nanoparticles cross the blood–tumor barrier, but are largely blocked by the normal blood–brain barrier, enabling high-resolution computed tomography tumor imaging. Gold radiation enhancement significantly improved long-term survival compared with radiotherapy alone. This approach holds promise to improve therapy of human brain tumors and other cancers.

Keywords

brain tumor; cancer; contrast agent; dose enhancement; glioma; gold nanoparticle; imaging; microcomputed tomography; radiotherapy; x-ray

[*]*Author for correspondence*: Tel.: +1 631 205 9490 Fax: +1 631 205 9493 hainfeld@nanoprobes.com.
[‡]Authors contributed equally

Financial & competing interests disclosure The authors have no other relevant relevant affiliations or financial involvement with any organization or entity with a financial interest in or financial conflict with the subject matter or materials discussed in the manuscript apart from those disclosed.

Ethical conduct of research The authors state that they have obtained appropriate Institutional Animal Care and Use Committee review board approval or have followed the princi ples outlined in the Declaration of Helsinki for all human or animal experimental investigations.

Every year, more than 22,000 people in the USA are diagnosed with primary brain tumors, with 13,000 deaths. The 5-year survival rate is 24%. Primary brain tumors account for 20% of cancers in children. However, metastases to the brain from other cancers are much more common, resulting in 130,000 deaths each year in the USA, accounting for 20% of all cancer deaths. New drugs and methods have yielded incremental advances and it is now recognized that cancer stem cells are particularly drug resistant [1]. Surgical intervention and radiotherapy provide only temporary life extension, especially for glioblastoma [2]. More effective treatments are desperately needed. Newer approaches include gene therapy, vaccine therapy, immunotherapy, locally applied venom toxin and ultrasound drug delivery [2–4].

A new approach involves the use of gold nanoparticles (AuNPs) to enhance radiotherapy [5–10]. High atomic number elements absorb x-rays efficiently and deposit this energy locally, mostly by the emission of photoelectrons, Compton scattering and Auger electrons. Similarly to using lead in order to shield radiation, gold also absorbs x-rays. This high atomic number local dose enhancement effect has been known for over 60 years [11]. Iodine was shown to increase the dose to cells in culture [12], and iodine contrast medium directly injected into tumors followed by kilovolt x-rays suppressed tumor growth in mice [13]. A CT scanner was modified to deliver tomographic 140 kVp x-rays to spontaneous canine brain tumors after intravenous (iv.) injection with iodine contrast medium and resulted in longer survival [14]. This apparatus was then used in a Phase I human trial of brain tumors using iv. injection of iodine contrast medium, which demonstrated the method to be safe and potentially beneficial [15]. Monochromatic synchrotron x-rays are currently being considered for iodine-enhanced treatment of brain tumors [16–18]. However, the difficulty with the low-molecular-weight iodine agents involves achieving a high enough concentration in tumors [16]. With respect to gold, a radiation enhancement of more than 100 was demonstrated in cells irradiated on a gold foil with a range of 10 μm [19]. Calculations indicated that if a tumor is loaded with gold at attainable levels, the local radiation dose can be at least doubled [20]. Micron-sized gold particles directly injected into tumors were tested, but did not disperse within the tumor [21]. However, 1.9 nm AuNPs iv. injected into mice with subcutaneous tumors followed by 26 Gy (250 kVp) x-rays led to 86% long-term survival (>1 year) compared with 20% survival with radiation alone [5]. Subsequent trials also demonstrated that AuNPs were effective in enhancing radiation treatment of tumors *in vivo* [22]. Many theoretical studies have also appeared studying the use of AuNPs for radiation enhancement. Herein, the use of iv. injected AuNPs for x-ray imaging and enhanced radiotherapy of an otherwise lethal intracerebral malignant mouse glioma is reported.

Methods & materials

Tumors & mice

A highly malignant brain tumor, Tu-2449, was chosen owing to its similarity to aggressive human gliomas [23,24]. A total of 5000 Tu-2449 cells derived from GFAP-v-src transgenic mice were implanted 2.5–3.0 mm deep at the middle of the left coronal suture of the skull into the striatum of syngeneic black B6C3f1 mice [24]. A total of 10 days later, tumors were 3–5 mm in diameter. AuNPs were injected via the tail vein at specified doses. For some mice, vardenafil (10 mg/kg) [25] was given orally by gavage 30 min prior to iv. injection of AuNPs. For therapy, mice were injected with AuNPs 9 days after tumor initiation and irradiated 15 h later. A total of 17 mice were used for AuNPs plus irradiation, 18 mice with radiation alone, ten mice with AuNPs alone and 18 mice with no treatment; all mice had implanted gliomas. Animal experiments were conducted according to NIH guidelines, and approved by the authors' institutional animal care and use committee before the start of the study.

Gold nanoparticles

AuNPs were obtained from Nanoprobes (NY, USA; Cat. No.: 1115), supplied as a 200 mg Au/ml solution in phosphate-buffered saline. Particles were further concentrated with a 100-kDa centrifugal filter (Millipore, MA, USA) to 400 mg Au/ml.

Electron microscopy

AuNPs were water washed using a 100-kDa filter to remove salt, diluted in 50% ethanol, applied to a carbon-coated grid, air dried and imaged in a FEI Tecnai™ G2 Spirit BioTWIN (FEI, OR, USA) transmission electron microscope operating at 120 kV. AuNP sizes were analyzed using ImageJ software [101].

MicroCT

A μCT40 and VivaCT 40 (SCANCO Medical AG, Brüttisellen, Switzerland) were used, operating at 45 kVp with 0.5 mm Al filtering, sampling with 15 × 15 × 15-μm voxels in a 30-mm diameter field. Three millimeter stacks of 200 sections at 2000 projections/revolution and an integration time of 300 ms/projection were collected, each stack requiring 20 min. Typical scans were 15 mm in length, thus taking 100 min. Images were quantified and presented using Amira® software (Mercury Computer Systems, MA, USA). Mice were anesthetized with isoflurane gas during imaging.

Irradiations

Mice were anesthetized with 140 mg/kg ketamine and 3 mg/kg xylazine in phosphate-buffered saline given intraperitoneally in approximately 0.06 ml. The head and body were protected by a 3.4-mm-thick lead shield with a notch that enabled irradiation 6.0 mm caudally from the posterior canthus of the left eyelid and dorsally from the dome of the palate to above the calvarium (Figure 1A). Irradiations were performed using an RT100 x-ray generator (Philips, Amsterdam, The Netherlands) operating at 100 kVp with a 1.7-mm Al filter. Dose was calibrated using an ion chamber (Radcal, CA, USA). To prevent lethal brain edema, dexamethasone (5 mg/kg) was injected intraperitoneally every 12 h starting on the day before irradiation, five times in total [26].

Gold quantification Microcomputed tomography

Concentrations of gold were measured from microcomputed tomography (microCT) images as previously described [27]. Briefly, standard gold solutions (0, 1, 2, 5, 10, 20 and 60 mg Au/ml) were placed in 1.5-ml Eppendorf tubes surrounded by water (15 mm in diameter). MicroCT intensity values were plotted versus concentration. The linear attenuation coefficient of the sample in Hounsfield units (HU) was plotted versus gold concentration using Equation 1:

$$\mathrm{HU} = 1000 \times (\text{image intensity} - \text{image intensity of water}) / \text{image intensity of water} \quad (1)$$

Mice without gold injection were scanned, in order to determine the average image intensity value of normal brain tissue. Image intensity from gold in the tumor showed a sharp decline outside the tumor and this edge was used to manually encircle the tumor for each scan section. The image intensity values were then integrated over either the whole tumor or equivalent volumes away from the tumor (for normal brain uptake) and averaged. The tissue intensity value from the normal brain without gold was subtracted from tumor intensity, and the difference was used to read from the calibration graphs to determine the gold concentration and HU. Six mice were analyzed for statistics.

Atomic absorption spectroscopy—For comparison and confirmation, four mice were imaged by microCT, then immediately dissected, placing brain tumor, normal brain tissue and other tissues in preweighed vials. Tissues were then digested with aqua regia and gold content measured by graphite furnace atomic absorption spectroscopy (PerkinElmer 4100Z, PerkinElmer, MA, USA).

Statistical analysis

Significance between treatment groups ($p < 0.05$) was assessed by a log-rank (Mantel–Cox) survival analysis test with 95% CIs using GraphPad Prism® software (GraphPad Software, Inc., CA, USA).

Results

The spherical AuNPs were imaged by electron microscopy and a statistical evaluation found a size distribution of 11.2 ± 8.6 nm. AuNPs were injected via the tail vein. After 4 h, necropsies revealed that the tumor had turned black due to AuNP uptake, whereas normal brain tissues remained pink (Figure 1B). MicroCT imaging further revealed highly specific tumor uptake of the AuNPs (Figures 2A–2C). A total of 15 h after iv. AuNP injection (corresponding to the time of irradiation), gold contrast was distributed throughout the tumor, but not homogeneously (Figures 2B & 2C). At earlier times (1 h, Figures2D–2F), gold could be seen escaping from the angiogenic blood vessels in the tumor, but not from vessels in normal brain tissue that had an intact blood-brain barrier. Tumor vessels 30 μm in diameter could be discerned. `Hot spots' (focal dots of gold accumulation) could also be seen (arrows, Figure 2E). Some tumor vessels showed segmental leakage (arrows, Figure 2F). The AuNPs accumulated in the tumor by the enhanced permeability and retention effect [28] and could be followed for several days after iv. injection (Figures 3A–3C). The AuNPs appeared to expand with tumor growth, albeit with dilution of intensity, but still defined the tumor boundary. Internal to the tumor, the AuNPs condensed from a more uniform distribution at day 1 (Figure 3A) to more focal spots at day 3 and later (Figures 3B & 3C).

In contrast to subcutaneous tumors, day 1 after iv. injection of the AuNPs, the distribution in these orthotopic brain tumors was distributed throughout the tumor including its center (Figure 4A) compared with the AuNP distribution in a subcutaneous tumor model, which showed iv. injected AuNPs predominantly at the peripheral growing edge with poor penetration into the tumor center after iv. injection (Figure 4B) [27].

Because the authors found that these AuNPs have an LD_{50} (lethal dose, 50%; the dose that kills 50% of the animals) of >5 g Au/kg in mice, the dose was increased to 4 g Au/kg. This resulted in a corresponding increase in tumor uptake (measured by calibrated microCT [27]) to 1.5 ± 0.2% w/w gold, to the authors' knowledge the highest gold concentration ever achieved in a tumor by iv. administration. For comparison, mice just after microCT were dissected and gold content was measured alternatively by atomic absorption spectroscopy. This gave a tumor uptake of 1.2 ± 0.1% w/w gold (10.0 ± 0.6% injected dose per gram of tumor), and a tumor-to-normal brain ratio of 18.8:1. The microCT showed higher tumor uptake (1.5 ± 0.2% w/w gold), probably due to some surrounding nontumor tissue included in the dissection/atomic absorption spectrometry measurement. The average increase in radiodensity of the tumor 15 h after AuNP injection was 1050 HU. The AuNP blood half-life was measured to be 24 h.

The 1.5% gold delivered to the tumor was calculated [20] to give a radiotherapeutic dose-enhancement factor of approximately 3.4. To test this, mice were iv. injected at this dose, and 15 h later, mounted (Figure 1A) and irradiated with 30 Gy using 100 kVp x-rays. Tumor volumes at treatment were 12–15% of the whole brain volume. Controls were: the same

irradiation without AuNPs; unirradiated, tumor-bearing mice; and tumor-bearing mice given AuNPs without irradiation. AuNP treatment without radiation (control) showed no abatement in tumor growth. Resultant survival rates are shown in Figure 5A. Radiation (without AuNPs) prolonged life, but all animals were dead by day 150. Radiation plus gold resulted in 50% long-term survival (>1 year). In a second experiment using 35 Gy, long-term survival was 56% with AuNPs plus radiation versus 18% with radiation alone (Figure 5B). Combining both experiments, the radiation plus AuNP treatments were statistically distinct from the radiation-only groups ($p = 0.014$).

Discussion

An important opportunity exists in radiotherapy: no tissues can survive a dose of approximately 90 Gy, but such a high dose cannot be used clinically due to ancillary damage. Boosting the dose specifically in the tumor above this threshold permits lower, sparing doses in surrounding tissue while delivering a completely ablative dose to the tumor. AuNPs provide a way to approximate this favorable condition. Being able to preferentially increase the radiation dose in the tumor by twofold or more compared with normal tissue would be highly desirable clinically.

Several factors may be improved upon in additional trials: in this preliminary study, tumor imaging for focusing the irradiation to just cover the tumor was not performed and irradiation was unidirectional. Intensity-modulated radiotherapy would minimize normal brain damage while focusing on the tumor; the optimal time to irradiate after AuNP administration was not explored. This could maximize the tumor-to-normal brain–gold ratio and further enhance results. Furthermore, the murine tumors used occupied a much larger fraction of the brain (Figure 2C) than do most human brain tumors undergoing therapy.

Images shown in Figures 2–4 were without vardenafil, but mice undergoing therapy were predosed with vardenafil since that had been reported to increase drug delivery to brain tumors. However, our subsequent preliminary study ($n = 3$) did not show a significant change in tumor or normal brain uptake of these AuNPs when vardenafil was used, perhaps due to the larger size of the AuNPs compared with low-molecular-weight drugs.

Several days after iv. AuNP injection, focal concentrations of gold appeared that may indicate regions of necrosis, allowing the AuNPs to pool. The distribution of gold after iv. injection was different in brain tumors compared with subcutaneous carcinomas. Gold was distributed throughout the brain tumor instead of localizing primarily to the periphery of subcutaneous tumors (Figure 4) [27]. This seems to indicate a difference in tumor and vasculature growth patterns, perhaps indicating that brain tumor cells are more migratory, thus not severely compressing central blood vessels, limiting internal blood flow.

The mechanism of this enhanced treatment is by the interaction of x-rays with gold, predominantly by absorption of x-rays, which ejects inner shell electrons (photoelectrons) and by Compton scattering, which also results in ejected electrons. These electrons can travel tens of microns, depositing dose along their paths. Furthermore, vacant shells are then filled with electrons from upper shells, which releases energy resulting in Auger electron emission that predominantly has a short range (nanometers) and fluorescent photon emission, some of which may escape typical tumor sizes. Such emissions cause ionizations and free radicals that then damage cells, much the same as the mechanism of x-rays interacting with water or tissue without gold. Gold by itself, without radiation, did not result in any measurable difference in tumor growth compared with control (untreated mice) (Figure 5A), indicating that this concentration of gold does not have a drug or toxic effect. It has also been reported that gold plus radiation is more effective with tumor cells compared

with normal cells [7], and that gold is effective in enhancing dose at megavoltages [29] where the photoelectric effect is very small, indicating that further study of the mechanism is warranted.

The magnitude of the effective dose enhancement predicted, approximately 3.4×for a tumor loading of 1.5% w/w gold, comes from the Monte Carlo analysis presented by Cho [20]. In that work, tumors were modeled with between 0.7 and 3% gold and a standard 140 kVp x-ray generator. The dose enhancement was linear over this range, yielding a value of 3.4 for 1.5% gold. The authors used 100 kVp, which would actually give a slightly higher dose enhancement due to the increased photoelectric effect at the lower beam energy.

For clinical use, AuNPs could provide the following benefits: accurate determination of tumor position for treatment planning; quantification of tumor and nontumor gold uptake to predict local x-ray doses; enable submillimeter spatial resolution for earlier diagnosis [27,30–32]; render microsurgical resection of tumors near clinically eloquent structures less difficult due to the intense tumor coloring [33]; and may only require a single irradiation for treatment (as performed here) instead of the usual lengthy fractionation regimen.

The main radiation enhancement by gold is attributable to secondary photoelectron production, which is best with orthovoltage x-rays (~100–400 kVp). However, these penetrate less than 6–25 mV x-rays currently used for radiotherapy. Nevertheless, calculations show that gold plus 150 kVp x-rays with 1% gold loading and a 10:1 tumor:nontumor ratio would be superior to 15 mV linear accelerator treatment for the majority of human brain tumors [9]. Other factors to be considered are whole-body clearance of AuNPs and their possible toxicity. While initial results indicate low toxicity for AuNPs [34–36], additional studies are indicated.

Targeting the AuNPs using antibodies [27,32], peptides or other agents could provide additional specificity for imaging and therapy. This new approach could also be combined with chemotherapy to enhance specific drug delivery through radiation-damaged tumor endothelium.

Conclusion

In summary, results from this mouse study demonstrate that: iv. injected AuNPs specifically localize in brain gliomas in a 19:1 tumor-to-normal brain ratio; the AuNPs enabled exquisite high-resolution tumor imaging by microCT; the amount of gold delivered was high enough to multiply a radiotherapy dose in the tumor by a calculated factor of approximately 300%; a single radiotherapy dose of 30–35 Gy resulted in an average of 53% long-term (>1 year), tumor-free survival compared with an average of 9% using radiation alone; and that this new method potentially provides a way to more effectively treat brain tumors and other cancers.

Future perspective

Nanotechnology continues to be an exploding field filling the gap between single molecules and micron-sized particles. For medicine, these constructs provide new materials with favorable pharmacokinetics for imaging, targeting, drug delivery and drug release not formerly possible. AuNPs are of interest due to the inherent low toxicity of gold, with the caution that some AuNPs may be toxic depending on their organic coating, size and other parameters. AuNPs are already being examined clinical trials as absorbers of near infrared for heating and ablating tumors, and as drug carriers using the biodistribution of AuNPs to target tumors. More AuNP constructs should be expected to enter into clinical use in future years. AuNPs enable exquisite high-resolution and high-contrast imaging of blood vessels, organs, tissues, tumors, lymph nodes, malformations and other structures, and their use as x-

ray contrast agents in animal studies should increase. However, for clinical use, problems with poor whole-body clearance (a problem with most nanoparticles), skin coloration at high doses and cost are current obstacles that need to be overcome, especially for diagnostic procedures and screening of asymptomatic persons. It may be expected that other high-atomic-number nanoparticles of lower cost will be developed in the coming years. For cancer treatment, these restrictions are relaxed and some level of harmless side effects or additional cost may be acceptable. The high level of radiation dose enhancement achievable in tumors demonstrated in this study and supported by theoretical calculations indicates that many tumors could be more effectively treated using AuNPs. Appropriate orthovoltage intensity-modulated radiation therapy sources for optimal treatment using AuNPs should be developed by x-ray device manufacturers once the benefits are confirmed by additional studies. High-current, orthovoltage x-ray generators suitable for AuNP therapy have, in fact, already been developed for airport baggage scanning. Tumor dose enhancement with high-Z nanoparticles is also obtained with particle beams such as protons [37] and with energy-matched brachytherapy seeds [38], and these applications should increase. Malignant brain tumors are fatal, but, as shown here, efficacious treatments appear feasible. Clinical translation should be evaluated, but must progress through the necessary critical evaluation steps, including showing efficacy in larger animals and humans, with more complete toxicity studies assuring safety.

Acknowledgments

The authors thank D Mitra, P Lin, F Furuya, W Liu, P Micca, D Sasso, V Diaz-Doran and D Adams for their assistance.

This work was supported in part by NIH grant 1R43CA134074 to J Hainfeld, who is a part owner of Nanoprobes, Inc.

No writing assistance was utilized in the production of this manuscript.

References

Papers of special note have been highlighted as:

■ of interest

■ of considerable interest

1. Beier D, Schulz JB, Beier CP. Chemoresistance of glioblastoma cancer stem cells: much more complex than expected. Mol. Canc. 2011; 10:128.
2. Mrugala MM, Adair JE, Kiem HP. Outside the box: novel therapeutic strategies for glioblastoma. Cancer J. 2012; 18(1):51–58. [PubMed: 22290258]
3. Liu HL, Yang HW, Hua MY, Wei KC. Enhanced therapeutic agent delivery through magnetic resonance imaging-monitored focused ultrasound blood–brain barrier disruption for brain tumor treatment: an overview of the current preclinical status. Neurosurg. Focus. 2012; 32(1):E4. [PubMed: 22208897]
4. Parvez T. Present trend in the primary treatment of aggressive malignant glioma: glioblastoma multiforme. Technol. Cancer Res. Treat. 2008; 7(3):241–248. [PubMed: 18473496]
4. Hainfeld JF, Slatkin DN, Smilowitz HM. The use of gold nanoparticles to enhance radiotherapy in mice. Phys. Med. Biol. 2004; 49(18):N309–N315. [PubMed: 15509078] ■ The first report of gold nanoparticle tumor radiotherapy enhancement *in vivo*.
6. Hainfeld JF, Dilmanian FA, Slatkin DN, Smilowitz HM. Radiotherapy enhancement with gold nanoparticles. J. Pharm. Pharmacol. 2008; 60(8):977–985. [PubMed: 18644191] ■■ Review of gold nanoparticle radiotherapy enhancement.

7. Kong T, Zeng J, Wang X, et al. Enhancement of radiation cytotoxicity in breast-cancer cells by localized attachment of gold nanoparticles. Small. 2008; 4(9):1537–1543. [PubMed: 18712753]
8. Kong G, Braun RD, Dewhirst MW. Hyperthermia enables tumor-specific nanoparticle delivery: effect of particle size. Cancer Res. 2000; 60(16):4440–4445. [PubMed: 10969790]
9. McMahon SJ, Mendenhall MH, Jain S, Currell F. Radiotherapy in the presence of contrast agents: a general figure of merit and its application to gold nanoparticles. Phys. Med. Biol. 2008; 53(20): 5635–5651. [PubMed: 18812647] ■■ Indicates which human tumors would be more favorably treated by gold nanoparticle-enhanced radiation therapy than by conventional radiotherapy.
10. Zhang SX, Gao J, Buchholz TA, et al. Quantifying tumor-selective radiation dose enhancements using gold nanoparticles: a Monte Carlo simulation study. Biomed. Microdevices. 2009; 11(4): 925–933. [PubMed: 19381816]
11. Spiers FW. The influence of energy absorption and electron range on dosage in irradiated bone. Br. J. Radiol. 1949; 22:521–533. [PubMed: 18147720]
12. Matsudaira H, Ueno AM, Furuno I. Iodine contrast-medium sensitizes cultured mammalian-cells to x-rays but not to gamma-rays. Radiat. Res. 1980; 84(1):144–148. [PubMed: 7454977]
13. Santos Mello R, Callisen H, Winter J, Kagan AR, Norman A. Radiation dose enhancement in tumors with iodine. Med. Phys. 1983; 10(1):75–78. [PubMed: 6843516]
14. Norman A, Ingram M, Skillen RG, et al. X-ray phototherapy for canine brain masses. Radiat. Oncol. Investig. 1997; 5(1):8–14.
15. Rose JH, Norman A, Ingram M, et al. First radiotherapy of human metastatic brain tumors delivered by a computerized tomography scanner (CTRx). Int. J. Radiat. Oncol. Biol. Phys. 1999; 45(5):1127–1132. [PubMed: 10613304]
16. Rousseau J, Adam JF, Deman P, et al. Intracerebral delivery of 5-iodo-2'-deoxyuridine in combination with synchrotron stereotactic radiation for the therapy of the F98 glioma. J. Synchrotron. Radiat. 2009; 16(Pt 4):573–581. [PubMed: 19535873]
17. Edouard M, Broggio D, Prezado Y, et al. Treatment plans optimization for contrast-enhanced synchrotron stereotactic radiotherapy. Med. Phys. 2010; 37(6):2445–2456. [PubMed: 20632555]
18. Adam JF, Joubert A, Biston MC, et al. Prolonged survival of Fischer rats bearing F98 glioma after iodine-enhanced synchrotron stereotactic radiotherapy. Int. J. Radiat. Oncol. Biol. Phys. 2006; 64(2):603–611. [PubMed: 16338098]
19. Regulla DF, Hieber LB, Seidenbusch M. Physical and biological interface dose effects in tissue due to x-ray-induced release of secondary radiation from metallic gold surfaces. Radiat. Res. 1998; 150(1):92–100. [PubMed: 9650606]
20. Cho SH. Estimation of tumour dose enhancement due to gold nanoparticles during typical radiation treatments: a preliminary Monte Carlo study. Phys. Med. Biol. 2005; 50(15):N163–N173. [PubMed: 16030374] ■ The first theoretical report of tumor radiotherapy enhancement using gold nanoparticles.
21. Herold DM, Das IJ, Stobbe CC, Iyer RV, Chapman JD. Gold microspheres: a selective technique for producing biologically effective dose enhancement. Int. J. Radiat. Biol. 2000; 76(10):1357–1364. [PubMed: 11057744]
22. Hainfeld J, Dilmanian F, Zhong Z, Slatkin D, Smilowitz HM. Gold nanoparticles enhance radiation therapy of a squamous cell carcinoma growing in mice. Phys. Med. Biol. 2010; 55:3045. [PubMed: 20463371] ■ Study documenting the efficacy of gold nanoparticle-enhanced radiotherapy.
23. Weissenberger J, Steinbach JP, Malin G, et al. Development and malignant progression of astrocytomas in GFAP–v-src transgenic mice. Oncogene. 1997; 14(17):2005–2013. [PubMed: 9160879]
24. Smilowitz HM, Weissenberger J, Weis J, et al. Orthotopic transplantation of v-src-expressing glioma cell lines into immunocompetent mice: establishment of a new transplantable *in vivo* model for malignant glioma. J. Neurosurg. 2007; 106(4):652–659. [PubMed: 17432718]
25. Black KL, Yin D, Ong JM, et al. PDE5 inhibitors enhance tumor permeability and efficacy of chemotherapy in a rat brain tumor model. Brain Res. 2008; 1230:290–302. [PubMed: 18674521]

26. Geraci JP, Sun MC, Mariano MS. Amelioration of radiation nephropathy in rats by postirradiation treatment with dexamethasone and/or captopril. Radiat. Res. 1995; 143(1):58–68. [PubMed: 7597145]
27. Hainfeld JF, O'Connor MJ, Dilmanian FA, et al. Micro-CT enables microlocalisation and quantification of Her2-targeted gold nanoparticles within tumour regions. Br. J. Radiol. 2011; 84(1002):526–533. [PubMed: 21081567] ■ The first *in vivo* report of antibody-targeted gold nanoparticles for imaging.
28. Noguchi Y, Wu J, Duncan R, et al. Early phase tumor accumulation of macromolecules: a great difference in clearance rate between tumor and normal tissues. Jpn J. Cancer Res. 1998; 89(3): 307–314. [PubMed: 9600125]
29. McMahon SJ, Hyland WB, Muir MF, et al. Nanodosimetric effects of gold nanoparticles in megavoltage radiation therapy. Radiother. Oncol. 2011; 100(3):412–416. [PubMed: 21924786]
30. Hainfeld JF, Slatkin DN, Focella TM, Smilowitz HM. Gold nanoparticles: a new x-ray contrast agent. Br. J. Radiol. 2006; 79(939):248–253. [PubMed: 16498039] ■ The first report of gold nanoparticles used as an x-ray contrast agent *in vivo*.
31. Popovtzer R, Agrawal A, Kotov NA, et al. Targeted gold nanoparticles enable molecular CT imaging of cancer. Nano Lett. 2008; 8(12):4593–4596. [PubMed: 19367807]
32. Reuveni T, Motiei M, Romman Z, Popovtzer A, Popovtzer R. Targeted gold nanoparticles enable molecular CT imaging of cancer: an *in vivo* study. Int. J. Nanomed. 2011; 6:2859–2864.■■ Another study demonstrating the targeting of tumors with gold nanoparticles conjugated to antibodies.
33. Veiseh M, Gabikian P, Bahrami SB, et al. Tumor paint: a chlorotoxin:Cy5.5 bioconjugate for intraoperative visualization of cancer foci. Cancer Res. 2007; 67(14):6882–6888. [PubMed: 17638899]
34. Qian X, Peng XH, Ansari DO, et al. *In vivo* tumor targeting and spectroscopic detection with surface-enhanced Raman nanoparticle tags. Nat. Biotechnol. 2008; 26(1):83–90. [PubMed: 18157119]
35. Shukla R, Bansal V, Chaudhary M, et al. Biocompatibility of gold nanoparticles and their endocytotic fate inside the cellular compartment: a microscopic overview. Langmuir. 2005; 21(23):10644–10654. [PubMed: 16262332] Study indicating the noncytotoxic, nonimmunogenic and biocompatible properties of gold nanoparticles.
36. Connor EE, Mwamuka J, Gole A, Murphy CJ, Wyatt MD. Gold nanoparticles are taken up by human cells but do not cause acute cytotoxicity. Small. 2005; 1(3):325–327. [PubMed: 17193451]
37. Kim JK, Seo SJ, Kim KH, et al. Therapeutic application of metallic nanoparticles combined with particle-induced x-ray emission effect. Nanotechnology. 2010; 21(42):425102. [PubMed: 20858930]
38. Cho SH, Jones BL, Krishnan S. The dosimetric feasibility of gold nanoparticleaided radiation therapy (GNRT) via brachytherapy using low-energy gamma-/x-ray sources. Phys. Med. Biol. 2009; 54(16):4889–4905. [PubMed: 19636084]

Website

101. NIH. ImageJ software. ImageJ analysis download (program freely available). http://rsbweb.nih.gov/ij/download.html

Executive summary

Background

- Current brain tumor treatments are poorly effective, resulting in many cancer deaths. Here, it has been demonstrated that by combining gold nanoparticles (AuNPs) with radiotherapy, long-term (>1 year), tumor-free survival from aggressive, imminently lethal, intracerebral gliomas could be obtained in mice.

Results

- In this study, the authors demonstrate that intravenously injected core-shell AuNPs specifically localize to brain gliomas compared with normal brain tissue in a mouse model.
- The large x-ray absorption coefficient of gold provides high-contrast tumor imaging by microcomputed tomography, revealing individual tumor blood vessels. Irregular tumor shapes are accurately delineated by the AuNPs. Glioma growth can be followed over the days following AuNP injection, showing that the AuNPs expand with the tumor boundary and become more condensed in the tumor interior.
- Tumor loading of AuNPs in these orthotopic gliomas was found to be initially distributed throughout the tumor, very different from subcutaneous tumors where AuNPs are largely confined to the tumor periphery.
- Without obvious toxicity, gliomas could be loaded with 1.5% gold by weight with a 19:1 glioma:normal brain ratio. This is calculated to give a radiation dose enhancement of approximately 300%.
- Application of 30 Gy at 100 kVp after intravenous injection of AuNPs resulted in 50% long-term (>1 year) survival compared with 0% survival with radiation only. A repeated experiment using 35 Gy gave similar results.

Discussion

- Potential drawbacks of this approach include long-term retention of some nanoparticles, especially in the liver, spleen and even in skin, and the high cost of gold. For therapy, high-power orthovoltage intensity-modulated radiation therapy machines need to be optimized for use with AuNPs.
- Clinical translation for brain tumor therapy in humans awaits testing in larger animals to further assess safety and efficacy.

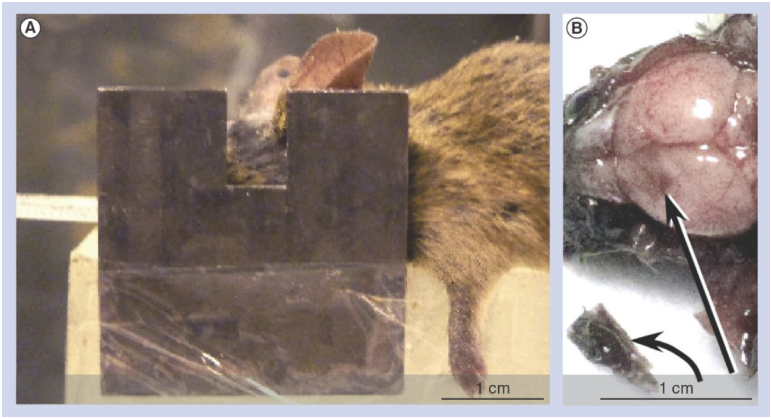

Figure 1. Irradiation and tumor dissection

(A) Irradiation setup showing mouse with a lead collimator. **(B)** Mouse brain and glioma at necropsy 10 days after tumor initiation and 4 h after gold nanoparticle intravenous injection (4 g Au/kg). The tumor (curved arrow) was removed (place of removal: straight arrow). The removed tumor was black compared with normal brain tissue due to gold nanoparticle uptake.

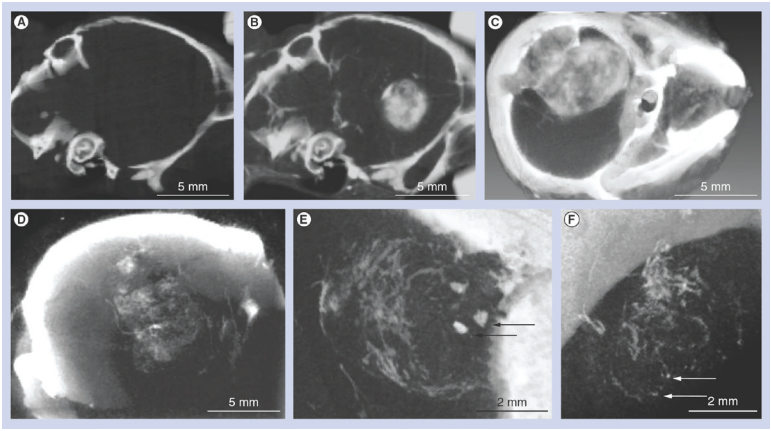

Figure 2. Microcomputed tomography imaging of brain tumors after intravenous gold nanoparticle injection

(A–C) Live mouse microcomputed tomography images of brain tumors 9 days postimplantation and 15 h after intravenous (iv.) gold nanoparticle (AuNP) injection. **(A & B)** Same mouse **(A)** before and **(B)** 15 h after iv. injection (4 g Au/kg). **(C)** Larger tumor imaged after iv. injection of 1.7 g Au/kg. **(D–F)** Live mouse microcomputed tomography images of a typical brain tumor 9 days postimplantation and 1 h after iv. AuNP injection (1.7 g Au/kg). **(D)** Individual blood vessels in the tumor could be discerned. **(E)** Focal spots of gold were also observed (arrows). **(F)** AuNP leakage was very irregular in some vessels (arrows).

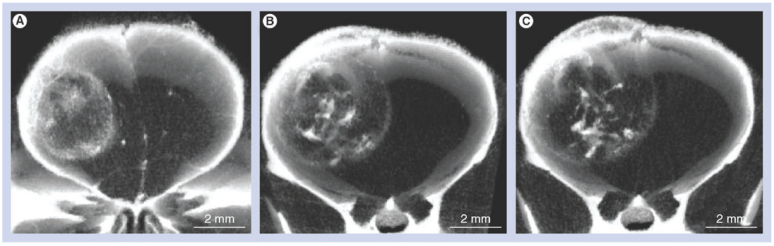

Figure 3. Tumor imaging time course over 8 days after intravenous gold nanoparticle injection

The same live mouse microcomputed tomography tumor images taken **(A)** 1 day, **(B)** 3 days and **(C)** 8 days after intravenous injection of gold nanoparticles (2 g Au/kg). Note how the gold expands with the tumor boundary, but becomes more punctuate and condensed internally. **(C)** Tumor is also infiltrating the scalp.

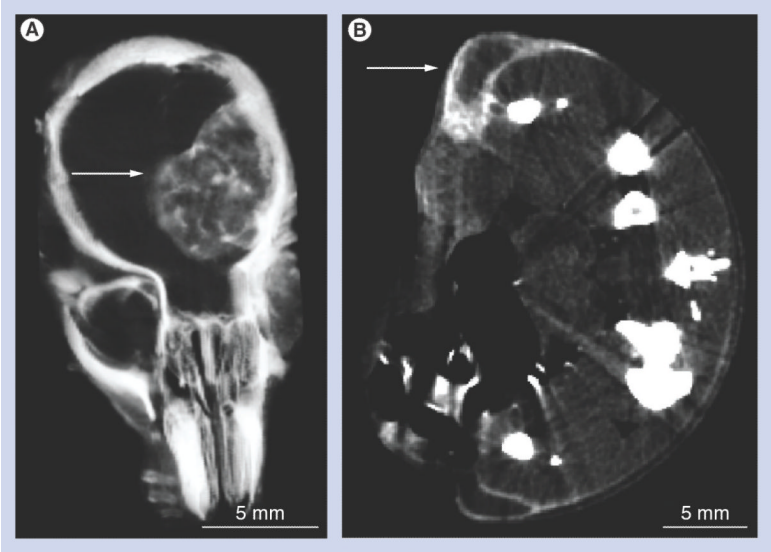

Figure 4. Microcomputed tomography sections comparing glioma versus subcutaneous tumor gold nanoparticle distribution after intravenous injection

Thin microcomputed tomography sections through the center of tumors of live mice bearing **(A)** an orthotopic brain tumor or **(B)** two subcutaneous tumors, one on each leg, see arrows. **(A)** Note how the gold nanoparticles (white contrast) are distributed throughout the brain tumor, even in its center, whereas **(B)** the subcutaneous tumors have gold nanoparticles predominantly at their periphery.

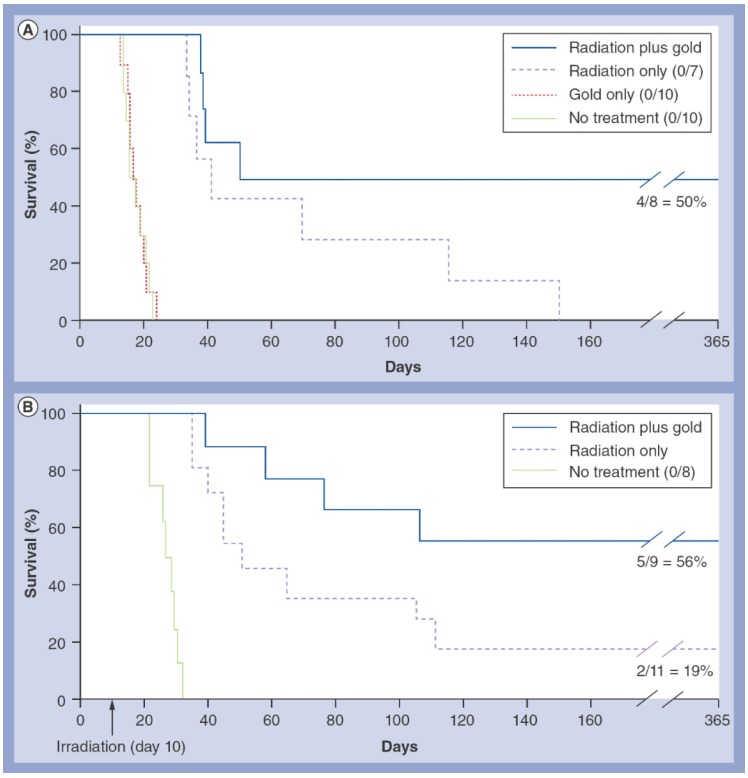

Figure 5. Kaplan-Meier survival graphs of mice with brain tumors after various treatments

(A) Groups: radiation only (30 Gy); radiation (30 Gy) plus intravenous (iv.) gold nanparticles (AuNPs; 4 g Au/kg); no treatment; and iv. AuNPs only (4 g Au/kg). Long-term survival (>365 days) was 50% in the gold plus radiation group (n = 8), and 0% in the untreated (n = 10), gold-only (n = 10) and radiation-only (n = 7) groups. **(B)** Repeat of experiment shown in **(A)**, except using 35 Gy instead of 30 Gy. Groups: no treatment; radiation only (35 Gy); and radiation (35 Gy) plus iv. AuNPs (4 g Au/kg). Long-term survival (>365 days) was 56% in the gold plus radiation group (n = 9), 18% in the radiation-only group (n = 11) and 0% in the untreated group (n = 8).